ELSEVIER

Ceramics International 29 (2003) 151–158

CERAMICS INTERNATIONAL

www.elsevier.com/locate/ceramint

Dense yttria stabilized zirconia: sintering and microstructure

Christel Laberty-Robert*, Florence Ansart, Céline Deloget, Manuel Gaudon, Abel Rousset

Centre Inter-Universitaire de Recherche et d'Ingénierie sur les Matériaux, CIRIMAT / LCMIE / UPS, Université Paul Sabatier, Bat II R1, 118 Route de Narbonne, 31062 Toulouse cedex 04, France

Received 20 November 2001; received in revised form 13 March 2002; accepted 14 May 2002

Abstract

Fine stabilized zirconia powders, which only contain small aggregates, were prepared by a modified Pechini process. These nanocrystalline powders, with an average crystallite size of 20 nm, were used to prepare dense ceramics. Resulting green microstructures and sintering behavior were studied. Green compacts of high green density were prepared by dry pressing and densified by a firing process. During firing, we have shown that dwell temperature and time significantly affected the final grain size and final density. However, a high final density ($> 98\%\ \rho_{th}$) and a final average grain size of 5 μm can be simultaneously achieved by controlling the sintering process. Indeed, the high densification was obtained by minimizing the grain growth that particles undergo when the sample is taken rapidly through the regime temperature in which surface diffusion predominates.

Keywords: D. ZrO_2; D. Y_2O_3; Ceramics; Chemical synthesis; Polymeric process

1. Introduction

Yttria stabilized zirconia (YSZ) is well known candidate for various applications such as oxygen sensors, fuel cells and catalytic membrane because of its good oxygen ionic conductivity and good mechanical properties at elevated temperatures [1]. In order to achieve high ionic conductivity, the material must be dense and uniform with a well controlled stoichiometry.

Recent studies made on stabilized zirconia have shown that the ionic conductivity may be influenced by the microstructure and the grain size. For example, the total ionic conductivity of 3 mol%Y_2O_3–ZrO_2 is mainly influenced by the grain boundaries rather the grain size [2]. Indeed, larger number of grain boundaries and porosity lead to greater resistivity in the fine grained samples. Additionally, the reduction of grain size in the ceramic also changes the mechanical properties and the sintering behavior of nanocrystalline materials [3,4]. The sintering temperature of nanocrystalline zirconia is about 400–500 °C lower than for microcrystalline material [5]. By lowering the sintering temperature, energy is saved and new opportunities for the co- sintering process of thin film devices arise. Up to now, it is easier to find in the literature articles referred small particles size (<1 μm) for yttria stabilized zirconia ceramic in the tetragonal phase. However, to our knowledge, it is difficult to stabilize fine grains of yttria stabilized zirconia ceramic in the cubic structure. Thus, the aim of this paper is on the synthesis of dense yttria stabilized zirconia ceramic (8%Y_2O_3–ZrO_2) with fine grains having the cubic phase.

For the synthesis of YSZ fine grains, the sol-gel process was used. Indeed, this method is a particularly attractive synthetic route for the preparation of fine inorganic powders, since a homogeneous mixture of the several components at a molecular level can be easily reached in solution [6–9,11]. In addition to greater homogeneity and purity of the product, the sol-gel method allows a low processing temperature and a morphological control of uniform crystalline particle size at superfine dimensions. In this paper, YSZ powders were prepared by a variant of the Pechini route [11] which is interesting for its simplicity, reproducibility, and easy scale-up. The powders have been characterized by X-Ray diffraction, thermal analysis, Transmission and Scanning Electron Microscopies. Then, these

* Corresponding author. Fax: +33-5-61-55-61-63.
E-mail address: laberty@iris.ups-tlse.fr (C. Laberty-Robert).

0272-8842/03/$22.00
PII: S0272-8842(02)00099-8

nanosize powders have been used for the elaboration of ceramics. The objective is to keep nanosize grains in the ceramic keeping the cubic symmetry. To succeed, the originality of the work is to propose a two step sintering process. This process allows us in a heating schedule to play on the difference in kinetics between grain boundary diffusion and grain-boundary migration. Dense yttria stabilized zirconia with fine grains in the cubic structure can be prepared.

2. Experimental

2.1. Powder synthesis

The nanocrystalline powders of yttrium-doped zirconia were prepared by the sol-gel method. Zirconium chloride $ZrCl_4$ and yttrium nitrate $Y(NO_3)_3,6H_2O$ were used as precursors for the citrate solution. Ethylene glycol and citric acid were used as polymerization/complexation agents for the process. The procedure for the preparation of yttria stabilized zirconia gel is outlined in the flow chart in Fig. 1. The raw materials used for YSZ synthesis are described in Table 1.

The citrate solution was prepared by dissolving appropriate ratios of zirconium (IV) chloride ($ZrCl_4$) and yttrium nitrate ($Y(NO_3)_3{\cdot}6H_2O$) in citric acid, as seen in Fig. 1. After homogenization of the solution containing cations, ethylene glycol was added, in CA/EG ratios of 5, 2.4, 1.2, 0.6 and 0.4 to promote mixed citrate polymerization by polyesterification reaction. By keeping the beaker on hot plate at a temperature of 80 °C under constant stirring, the solution became more viscous and a transparent gel was formed without any visible phase separation. This gel was then dried at 180 °C in air during a night. This material is called dried gel. Calcination of the dried gel at 400 °C in air was performed before final sintering in air at various temperatures (600, 800, 1000 °C) for 6 h in a muffle furnace Adamel CT5HT equipped with a West programmer. The final temperature is reached with a constant rise speed of 10 °C/h, and the calcination temperature is maintained at this temperature during 2 h. The thermal processing of sintering is carried out in a high temperature muffle furnace Nabertherm (maximum temperature 1600 °C). It is equipped with a programmer Eurotherm.

2.2. Materials characterization

TGA and DTA were performed on dried YSZ gels, which were prepared by heating it to 180 °C until solidification. Thermogravimetric experiments were performed in a vertical plug flow differential reactor. The mass variation was followed with a Cahn D200 microbalance (accuracy 10^{-6} g). A furnace monitored by a Shimaden SR25 temperature programmer can linearly

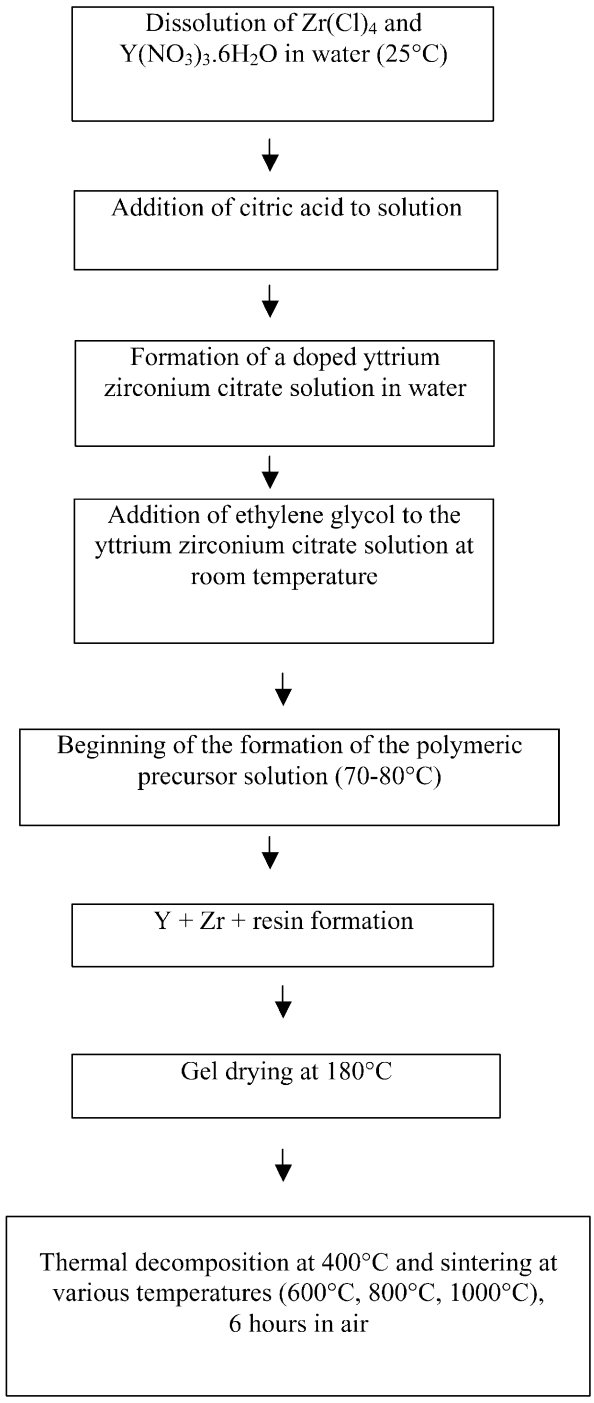

Fig. 1. A flow chart illustrating the processing procedure for the preparation of $8\%Y_2O_3$-ZrO_2.

Table 1
Raw materials used in the YSZ synthesis

Material	Source	Purity
Zirconium (IV) chloride ($ZrCl_4$)	Merck	>98
Yttrium nitrate ($Y(NO_3)_3.6H_2O$)	Aldrich	99.9
Citric acid	Aldrich	99
Ethylene glycol	Prolabo	99

increase the temperature of the sample. The YSZ gel was first pumped (10^2 Pa) at room temperature for 1 h and the apparatus was filled with air atmosphere. The temperature was then linearly increased until 1273 K (with a heating rate $\beta = 5$ K min^{-1}) and maintained at 1273 K during 1 h. TGA-mass spectra of the dried gel were measured in vacuum (10^{-6} mbar) using a thermobalance equipped with a Balzers QMG 421 mass spectrometer under a heating rate of 5 °C/min. The same procedure as thermal analysis (TGA and DTA) has been used.

X-ray diffraction (XRD) profiles were obtained using Cu-K_α radiation (SIEMENS D501) source to determine the crystallinity of the YSZ powder. The mean diameter of crystallites was determined from X-ray diffraction line broadening using the Scherrer formula [12]. Scanning electron microscopy (Jeol JSM 6400) and transmission electron microscopy were used to characterize the morphology and the microstructure of the YSZ powders. BET surface areas of the powders were measured using a Micrometrics Model 2100E Accusorb instrument. The porosity of the powders was estimated by means of a mercury porosimeter (MICROMERITICS Auto Pore II 9220) reaching 414 MPa and allowing the characterization of pores in the range of 360–0.003 μm.

Then, the measurement of the material withdrawal versus time during one sintering cycle is carried out using an electronic dilatometer NETZCH 402 E. A programmer controls the thermal cycle of the furnace and a processing system manages the data recording. This technique makes it possible to study the curves of ΔL/Lo withdrawal according to the temperature, like their derived curves with $\Delta L = L - L_o$ (L: length at time t, L_o: length at time $t = 0$).

The evaluation of the density of green and sintered pellets, was made by weighing and measurement of samples. The weighing is carried out on a Sartorius balance with an accuracy of 0.01 mg. Measurement is made using the Mitutoyo micrometer (accuracy: 0.001 mm). In practice, the experimental densities are compared with the theoretical densities. These last ones are calculated starting from the knowledge of the YSZ lattice parameters.

3. Results and discussion

3.1. Powder synthesis and morphology

Thermal analyses curves of the 200 °C dried powders obtained by the derivated Pechini process have been studied [13] and it has been shown that thermal decomposition is completed at 400 °C and several steps occur. Mass spectrometry analyses showed that the different steps cannot be attributed in a simple manner, each step corresponds to the formation of several gases CO, CO_2 and NO.

The XRD patterns of the powders calcined at various temperatures are reported on Fig. 2. The significant line broadening that may be observed in the XRD spectra of the powder indicates that powders consist of crystallites with a diameter $\leqslant 100$ nm. Standard X-ray line broadening measurement shows that the crystallites have a diameter smaller than 30 nm. Further, Table 2 illustrates the influence of the heating temperature on the crystallite size. It can be seen from this table that the crystallite size of ZrO_2-8%molY_2O_3 powders increases as the heating temperature increases. Under the experimental conditions studied, powders calcined at 400 °C possess the smallest crystallite size of about 3 nm while

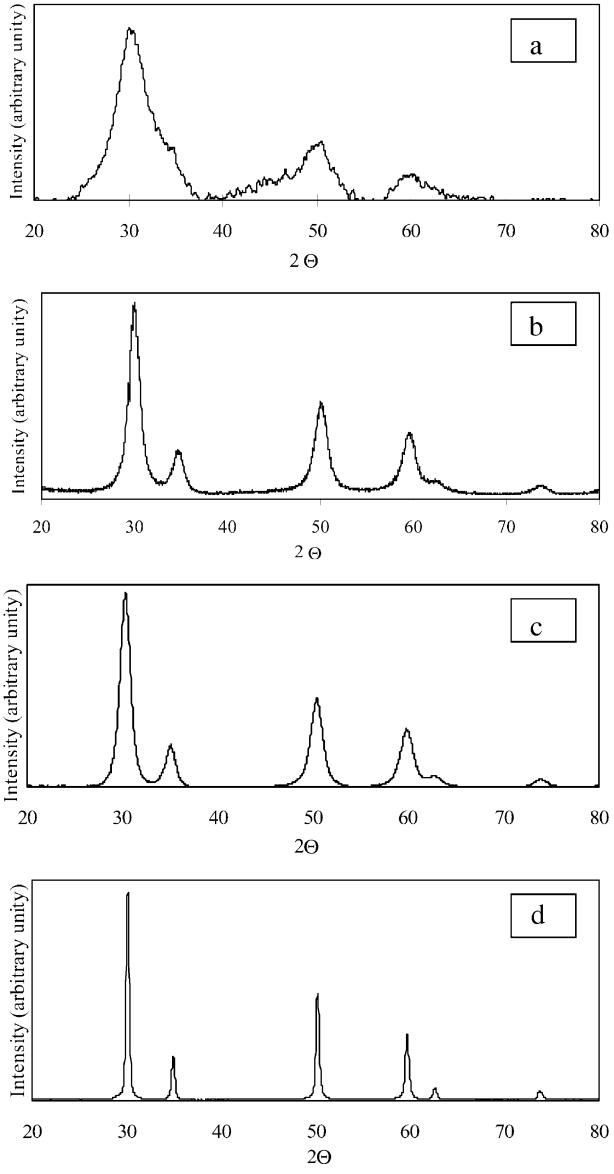

Fig. 2. Powder X-ray diffraction patterns (Cu-Kα) of YSZ samples calcined at (a) 320 °C, (b) 400 °C, (c) 600 °C, (d) 1000 °C.

Table 2
Specific surface area, particles size evaluated from XRD analysis and calculated from BET measurements

Calcination temperature (°C)	Crystallites size (nm) from XRD analysis	Specific surface area (m^2/g)	Crystallites size (nm) evaluated from BET measurements
400	3±2	39±4	18
600	5±1	30±3	21
700	6±2	26±3	24
800	7±2	18±2	28
1000	26±5	10±1	37

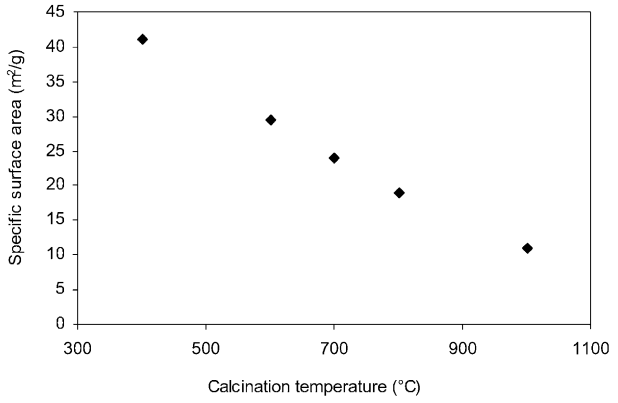

Fig. 3. BET measurements of ZrO_2-8%Y_2O_3 powders as a function of the calcination temperatures.

the crystallite size is increased to about 30 nm when heating temperature of 1000 °C is used.

The calcination temperature affects both crystallite size and specific surface area of the powders (Fig. 3, Table 2). As observed, crystallite growth of yttria stabilized zirconia is enhanced by the calcination temperature. The mean crystallite size ranges from 3 to 30 nm showing that the method is effective to synthesize nanosized powders.

Specific surface areas decreased with increasing the heating temperature. For example, the sample calcined at 400 °C has the highest specific surface area in the series. However, upon calcination at 1000 °C, its specific surface area is reduced by a factor 4. This seems to be mostly due to the reduction in bulk porosity of the compound [13].

A comparison of particle size evaluated from XRD analysis and specific surface area measurements shows that particles are agglomerated. The size of particles and agglomerates increases with the heating temperature; A factor 4 between agglomerated and particle size is observed up to 800 °C. At 1000 °C, the difference is lower.

In addition, it can be seen that the specific surface area of the calcined powders regularly decreases when the calcination temperature goes up and the crystallite size of the powders increases. This strengthens the tendency to form a dense structure in the agglomerate and hence the specific surface area comes down.

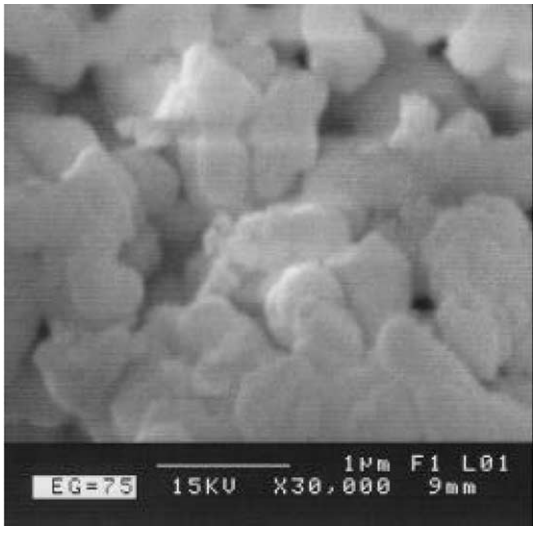

Fig. 4. SEM features of YSZ powders calcined at 1000 °C.

Scanning electron microscopy studies confirm in powders the presence of agglomerates (Fig. 4). Preliminary TEM studies of powders calcined at 1000 °C show a partial sintering of the primary crystallite (Fig. 5). This results is also observed during the synthesis of yttria stabilized zirconia by a combustion process [14].

In Fig. 6 is reported the porous distribution as a function of the pore diameter for 8%Y_2O_3-ZrO_2 powders. As it can be seen, powders present two pore distributions, one centered on 10 μm and the other one on 0.1 μm. This result shows that powders obtained via the Pechini process are porous.

Then, pure nanocrystalline yttria stabilized zirconia can be prepared by a tailored Pechini process. The very fine crystallite sizes obtained lead to the stabilization of the cubic phases at room temperature.

To study the compact behavior of YSZ ceramics, powders synthesized for a CA/EG ratio of 2.4 at 1000 °C and having particles size of about 20 nm have been used.

3.2. Sintering behavior

A YSZ compact is illustrated in Fig. 7. The SEM micrograph is representative of the packing in the powder

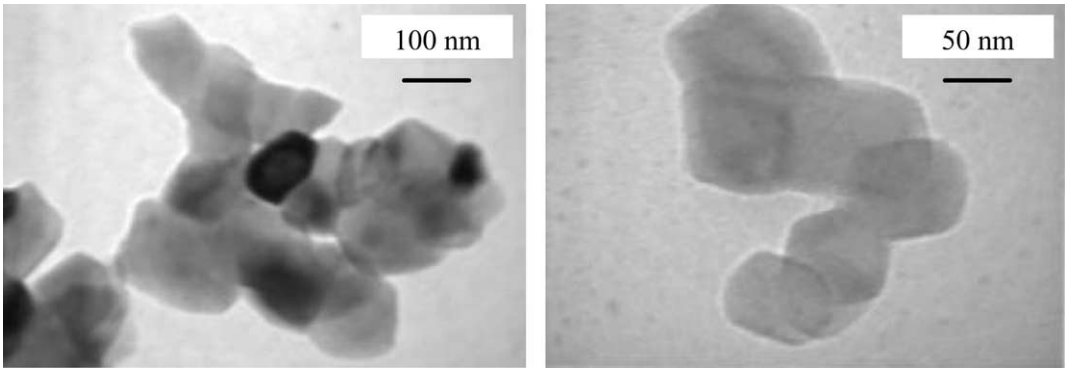

Fig. 5. TEM features of powders calcined at 1000 °C.

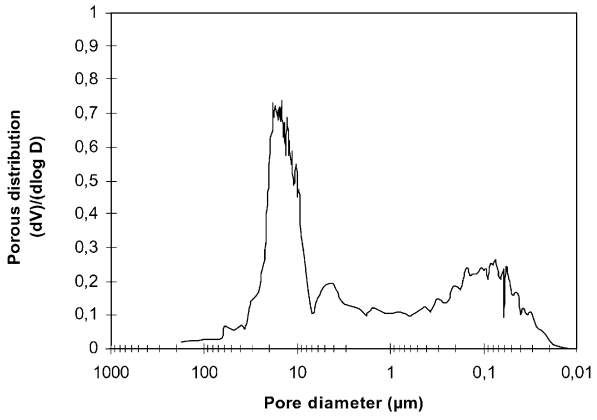

Fig. 6. Porous distribution as a function of pore diameter for the 8%Y_2O_3-ZrO_2 powders.

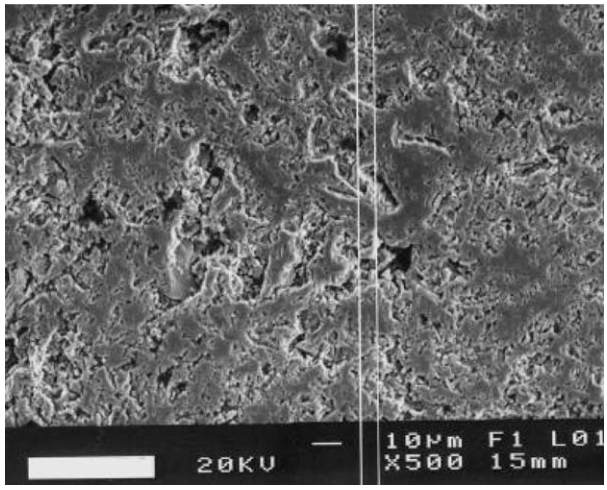

Fig. 7. Scanning electron micrograph of YSZ ceramic made from YSZ powders calcined at 1500 °C.

compacts. For this compound, the relative density is about 88%.

In order to estimate the hardness of the agglomerate and the best experimental conditions, YSZ powders calcined at 1000 °C were uniaxially cold pressed up to 16 tons. The relative green densities as a function of the compaction pressure are represented in Fig. 8.

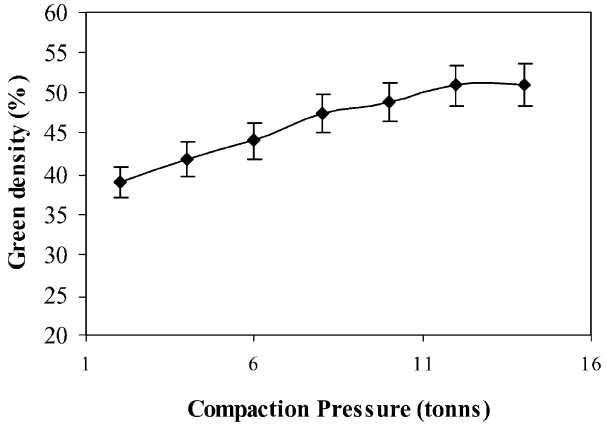

Fig. 8. Green density versus compaction pressure for 8%Y_2O_3-ZrO_2 powders.

Increasing compaction pressure favors the densification as shown in this figure. The density increases from 35 to 50% of theoretical densities with increasing the compaction pressure from 2 to 11 tons. However, for compaction pressure in the range [12 tons; 14 tons], the green density remains stable. But, for compaction pressure up to 14 tons, a decrease in green density is observed. Then, a compaction pressure of 11 tons which conduces to green density of about 50% is used in the following study. In addition, the influence of the pressure time for this compaction pressure on the green density has been investigated and no influence was observed.

The linear shrinkage rate of powder compacts, sintered in a dilatometer with a constant heating rate of 5 °C/min is illustrated in the curve of Fig. 9. The curve presents two peaks of the shrinkage rate.

This behavior suggests that aggregates are present. Elimination of the intra-aggregate pores during the sintering corresponds to the lower-temperature peak. In addition, in this temperature area, an increase in grain growth is observed and is mainly due to grain growth within these small aggregates. The relatively regular and dense internal packing situation in these agglomerates provides a large number of necks, formed during

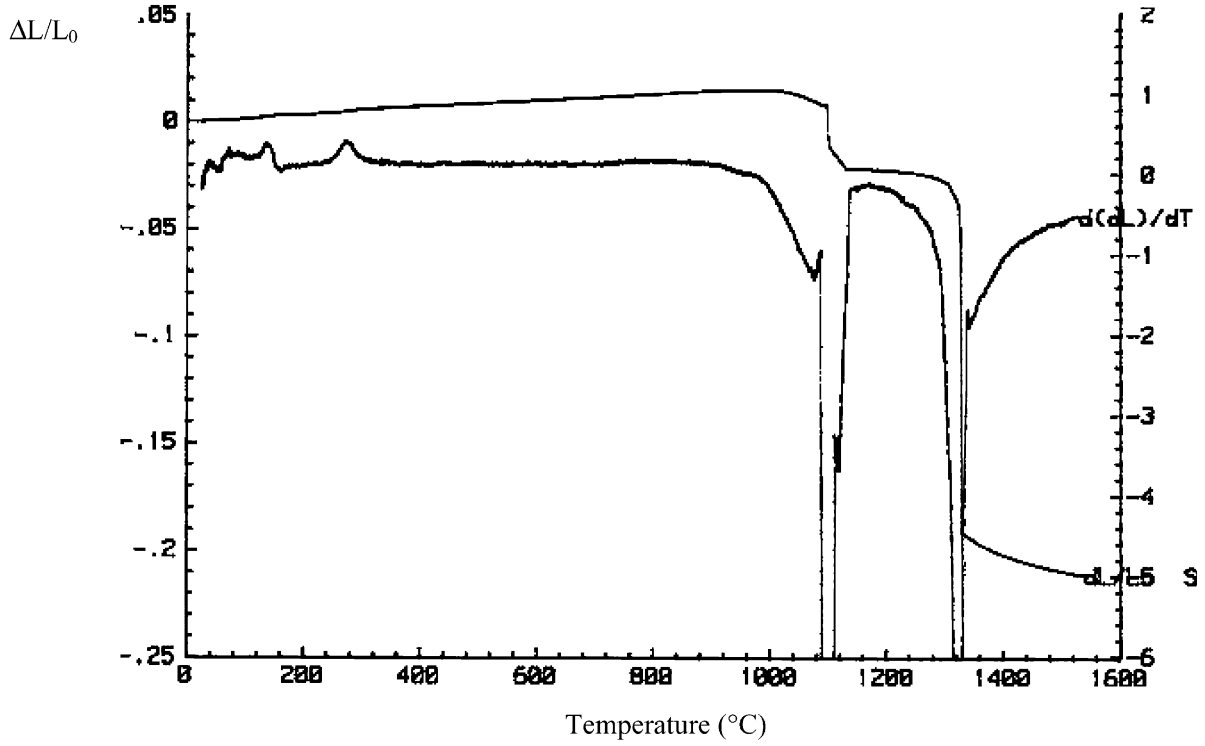

Fig. 9. $\Delta L/L_o$ as a function of the sintering temperature.

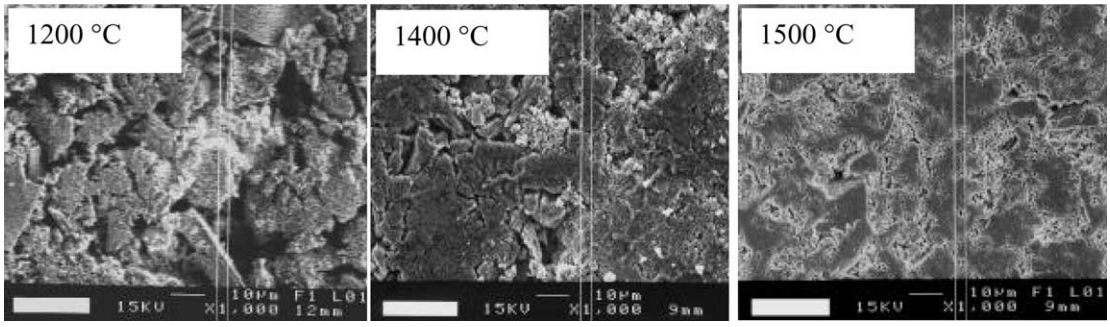

Fig. 10. Grain growth and densification behavior during sintering.

calcinations, between the primary crystallites. According to Van de Graaf [15], these packings situation may lead to fast sintering and the achievement of full density at low temperature. After sintering at 1000 °C, it can be observed an increase of the particles and aggregates size (Fig. 10).

This observation means that no significant overall shrinkage appears in this stage of the sintering process. For temperature ranging from 1200 to 1400 °C, the densification is connected to the inter-aggregate pore elimination. Indeed, it can be observed that grain growth accelerates strongly in this area. A study of the variation of the relative densities as a function of the sintering temperature has been reported in Fig. 11. The densification increases with the sintering temperature. However, the resultant densification of the whole body is poor (90%) and complete densification > 95% is not reached.

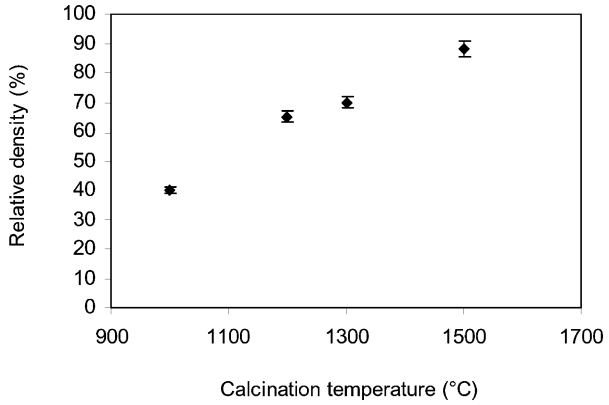

Fig. 11. Evolution of the relative densities as a function of the sintering temperature.

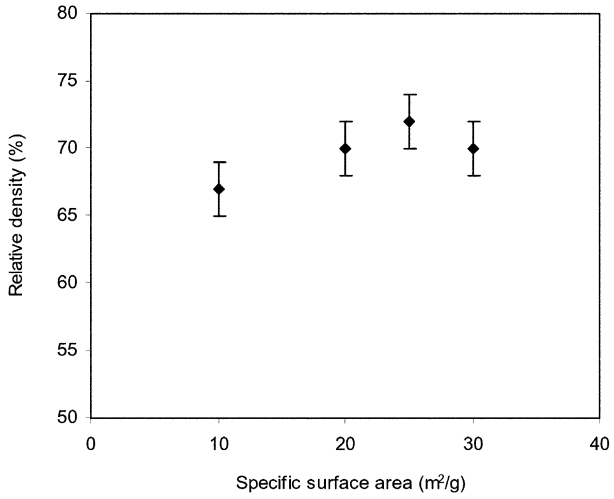

Fig. 12. Evolution of the relative densities as a function of the agglomerate sizes in the starting powders, sintering temperature is 1450 °C.

According to Quinelato work's [16], a correlation exists between the microstructure of the green compact and the density of sintered compact. Usually complete densification in the sintered compact is obtained for high degree of homogeneity of the packing green compact. This is linked to the nature of the powders and may be achieved when powders have small crystallites size and are unagglomerated. Though, using wet-chemical routes, it is very difficult to obtain non agglomerated submicronic powders. Roosen's work [17] showed that the nature of the agglomerate influences the pores size in the green body. Densification is high when a powder consisting of soft agglomerates is compacted. In our case, it seems that the powders consist of soft agglomerates. The relative density for powder having various agglomerate size has been studied and results are reported in Fig. 12. There is no variation of the density with the average of the agglomerate size. This pointed out that during compaction, the agglomerates can be destroyed at relatively low pressures and form inter and intra agglomerate pores of same size with a narrow pore size distribution which can be eliminated by sintering.

According to Chen's work on cubic Y_2O_3 oxides, a final density of aggregates powders of 98% can be reached by using in a heating schedule the difference in kinetics between grain-boundary diffusion and grain-boundary migration [18]. Accordingly, the sample is first heated at a higher temperature to achieve an intermediate density, then cooled down and held at a lower temperature until it was fully dense. In Fig. 13 is reported the grain growth size of YSZ in two-step sintering. It can be seen that full density was achieved when YSZ ceramic was first heated at 1500 °C and then after holding at 1450 °C for 20 h (Fig. 14). This result is different from those of Fig. 10 (heating schedule in one step) showing for a final sintering at 1500 °C a relative density that not exceed 90%. However to succeed in two steps sintering, a sufficiently high starting density should be obtained during the first step. Indeed, Chen et al. [19,20] showed that, when the density is above 70%, porosimetry data have shown that all pores in Y_2O_3 become subcritical [19–21] and unstable against shrinkage. Then, even if the particles network is frozen, as it is obvious in the second step, these pores can be filled as long as grain boundary diffusion allows it. In our study, densities higher than 80% were necessarily for second step sintering. Indeed, for YSZ initially heated to 1300 °C, density of 90% was achieved after holding at 1250 °C for 20 h. Thus, the ceramic is not fully densified. In order to control grain growth, the dwelling time at 1450 °C have been studied. Results have been reported

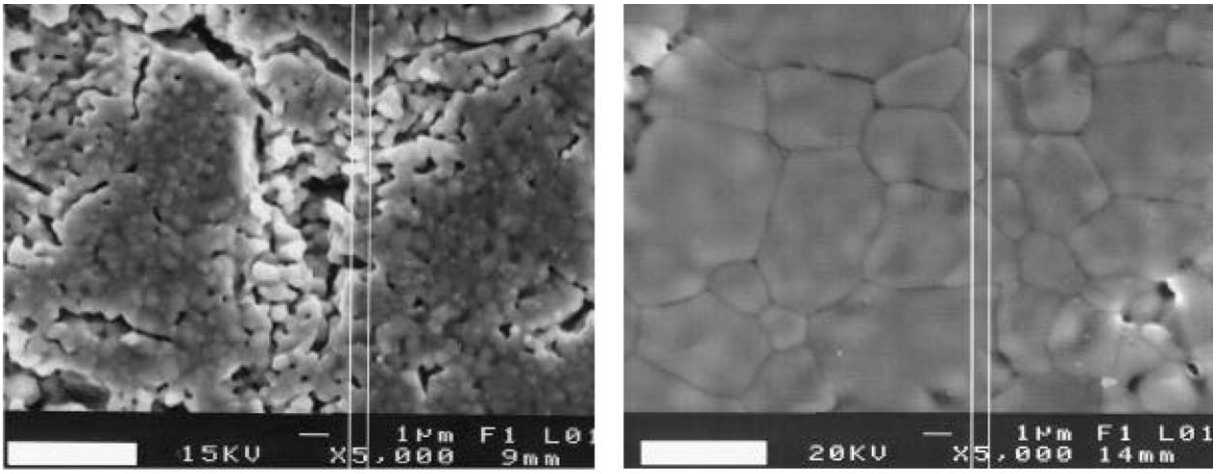

Fig. 13. Grain size of YSZ in two step sintering.

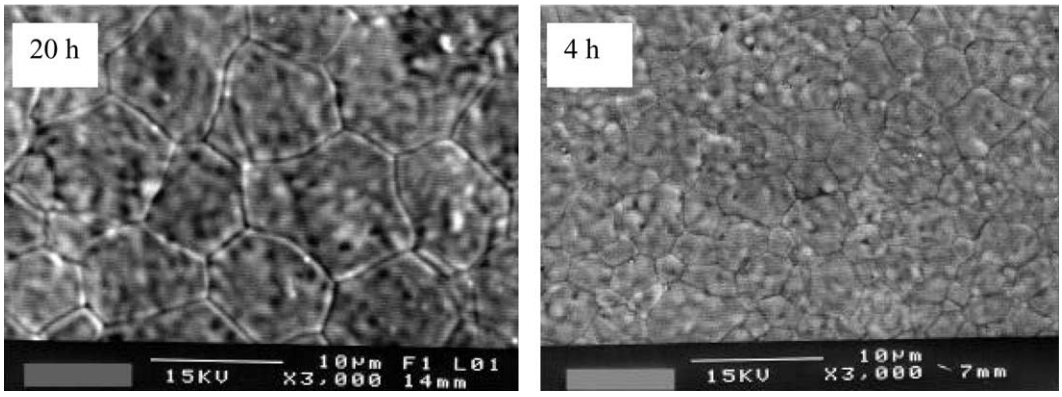

Fig. 14. Influence of the dwelling time at 1450 °C on the particle size.

on Fig. 14. As it can be seen, the dwelling time at 1450 °C plays an important role on the particle size (see Fig. 14). For a short dwelling time of 4 h, the particle size is smaller. The grain size of fully dense ceramics lies around 5 μm (see Fig. 14), and is about 10 times more than the starting powder size. This increase is mostly due to the coarsening in the first step sintering.

4. Conclusions

Nanocrystalline YSZ powders were synthesized using a modified Pechini process. The influence of synthesis parameters during thermal treatment on the characteristics of the powders (specific surface area, porosity, grain size, and agglomeration) was studied. Powders as small as 50 nm were obtained with narrow distribution and low porosity. These nanocrystalline samples were used to prepare YSZ compacts. The compaction pressure and time and the sintering behavior had an effect on the relative density of the ceramic and the average grain size. It was determined, that a high density ($> 98\%$ ρth) and fine average grain size ($=5$ μm) could be simultaneously achieved when a two steps sintering process was used. The high densification was due, in part, to the formation of subcritical pores in the ceramics during the first step. The sample was taken through high temperature (1500 °C) where grain boundary migration predominates. This densification is also due to the reduced coarsening that particles underwent during the second step when the temperature of the sample decreases to 1450 °C where grain boundary diffusion predominates. On the other hand, the final grain growth is achieved by the exploitation of the difference in kinetics between grain-boundary diffusion and grain-boundary migration.

References

[1] B.C.H. Steele, in: T. Takahashi (Ed.), High Conductivity Solid Ionic Conductors, Recent Trends and Applications, World Scientific, Singapore, 1989, p. 402.
[2] R. Ramamoorthy, D. Sundararaman, S. Ramasamy, Solid State Ionics 123 (1999) 271–278.
[3] M.J. Verkerk, B.J. Middelhuis, A.J. Burgraaf, Solid State Ionics 6 (1982) 159.
[4] N.M. Beckmans, L. Heyne, Electrochem. Acta. 2 (1976) 303.
[5] M. Yoshimura, Ceram. Bull. 67 (1988) 1950.
[6] T. Okubo, H. Nagamoto, J. Mater. Sci. 30 (1995) 749.
[7] T. Hours, P. Bergez, J. Charpin, A. Larbot, Am. Ceram. Soc. Bull. 71 (2) (1992) 200.
[8] P.H. McCluskey, G.S. Fischman, and R.L. Snyder, in: H. Hausner, G.L. Messing, S. Hirano (Eds.), Proc. 2nd Int. Conf. On Ceramic Powder Processing Science, 1989, p. 111.
[9] L.W. Tai, P.A. Lessing, J. Mater. Res. 7 (2) (1992) 502.
[11] M. P. Pechini, Patent, 11 July (1967) 3.330.697.
[12] H. Klug, L. Alexander, X-ray Diffraction Procedures, John Wiley, New York, 1962.
[13] Ch. Laberty-Robert, F. Ansart, C. Deloget, M. Gaudon, A. Rousset, Mater. Res. Bull. 36 (12) (2001) 2083.
[14] K.R. Venkatachari, D. Huang, S.P. Ostrander, W.A. Sculze, G.C. Stangle, J. Mater. Res. 10 (3) (1995) 748.
[15] M.C. Van De Graaf, T. Van Dicjk, M.A. De Jonjh, A.J. Burgraaf, Sci. Ceram. 9 (1977) 75.
[16] A.L. Quinelatelo, E. Longo, L.A. Perazolli, J.A. Varela, J. Eur. Ceram. Soc. 20 (2000) 1077.
[17] A. Roosen, H. Hausner, Techniques for agglomeration control during wet-chemical powder synthesis, Adv. Ceram. Mater. 3 (2) (1988) 131.
[18] I. Wei Chen, X-H. Wang, Nature 404 (2000) 168.
[19] P.L. Chen, I-W. Chen, J. Am. Ceram. Soc. 79 (1996) 3129.
[20] P.L. Chen, I-W. Chen, J. Am. Ceram. Soc. 80 (1997) 637.
[21] W.D. Kingery, B. Francois, in: G.C. Kuczynski, N.S. Hooton, C.F. Gibbon (Eds.) Sintering and Related Phenomena, Gordon Breach, New York, 1967, pp. 471–496.